PHYSICAL REVIEW C VOLUME 50, NUMBER 5 NOVEMBER 1994

Role of the supersymmetric semiclassical approach in barrier penetration and heavy-ion fusion

T. Sil and R. Dutt
Department of Physics, Visva-Bharati University, Santiniketan 731 235, West Bengal, India

Y. P. Varshni
Department of Physics, University of Ottawa, Ottawa, Ontario, Canada K1N 6N5
(Received 27 May 1994)

The problem of heavy-ion fusion reactions in the one-dimensional barrier penetration model (BPM) has been reexamined in light of supersymmetry-inspired WKB (SWKB) method. Motivated by our recent work [Phys. Lett. A **184**, 209 (1994)] describing the SWKB method for the computation of the transmission coefficient $T(E)$, we have performed similar calculations for a potential barrier that mimics the proximity potential obtained by fitting experimentally measured fusion cross section $\sigma_F(E)$ for the light-light and light-heavy systems. For illustration, we have first dealt with an analytically solvable potential which interpolates between two well-known nuclear barriers such as the Morse and the Eckart for two limiting values of the free parameter of the potential. Comparison of the predicted $T(E)$ with the exact analytic ones reveals that the present scheme yields consistently better results than those obtained from the WKB approximation. Furthermore, in contrast to the WKB method, analytic continuation of our SWKB transmission coefficient for the corresponding potential well (obtained through the inversion procedure) leads to exact energy eigenvalues. We have further studied the energy dependence of the total fusion cross section for different processes such as $^{16}O+^{12}C$, $^{19}F+^{12}C$, $^{16}O+^{208}Pb$, and ^{16}O with even isotopes of Sm, using a parametrized potential barrier suggested by Ahmed. The predicted cross sections are in agreement with values obtained from the WKB method and with direct experimental measurements for the beam energy near and above the Coulomb barrier. In the case of sub-barrier fusion, our results are substantially better than those given by the Hill-Wheeler parabolic approximation which overestimates $\sigma_F(E)$, especially for the light-ion systems.

PACS number(s): 24.10.−i, 25.70.Jj

I. INTRODUCTION

The study of heavy-ion fusion has received wide attention in recent years due to the fact that the fusion cross section σ_F can give information on nuclear structure as well as on the formation of quasimolecular resonances [1–4]. In the past, such studies were not possible due to the experimental difficulties in measuring very small values of σ_F for sub-barrier fusion. In recent experiments, the fusion cross sections can be measured with good accuracy for nuclei with a wide range of mass numbers and energy of the projectile. Experimentally large numbers of data are now available for light-light and light-heavy nuclei in both the sub-barrier and above-barrier fusion [4–8].

To the theorists it remains a challenge as to how well the experimental data can be explained by potential model calculations. Obviously, the theoretical models are bound to be complicated due to the complex nature of the structure of the colliding nuclei and the presence of many different reaction channels [9–11]. For example, it was observed [5,12] that the fusion cross sections of very similar systems differing from one another by one or two nucleons only, such as $^{12}C+^{12}C$, $^{12}C+^{13}C$, and $^{13}C+^{13}C$, exhibit substantially different energy dependence of $\sigma_F(E)$ at sub-barrier energies. This clearly indicates that one must consider details of the nuclear structure, namely, the effect of permanent deformation of interacting nuclei, zero point oscillation of the nuclear shape, neck formation, etc. so as to explain the behavior of the fusion excitation function correctly at low energies [13–15].

The simplest theoretical way of understanding the fusion of two nuclei is the barrier penetration model (BPM) where the projectile ion is assumed to penetrate through the mutual potential barrier between two interacting nuclei and to form a composite nucleus. The effective interaction barrier is given by

$$V_{\text{eff}}(r) = V_N(r) + V_C(r) + V_{\text{cent}}(r), \qquad (1.1)$$

which is composed of nuclear, Coulomb, and centrifugal interactions. The shape of the barrier depends on the choice of the nuclear and the Coulomb potentials. The main trick in the theoretical approach lies in obtaining an optimum form of the nuclear potential which is the only component in (1.1) that contains free parameters. Several attempts [1,16,17] based on model calculations were made to explain the measured cross sections. The standard potential of Woods-Saxon form with deep real and imaginary parts was first obtained by Reeves [18] by fitting the $^{12}C+^{12}C$ low energy data. However, this model did not work out nicely for other systems, such as $^{16}O+^{16}O$, indicating that different global potentials may behave differently with change in the atomic and mass numbers, Z and A. Subsequently, Blocki *et al.* [19] proposed a form of $V_N(r)$ known as proximity potential derived in a very general way for leptodermous (thin skinned) systems. The gross structure of the fusion cross section may be well accounted for by assuming

$$\sigma_F(E) = \sum_{l=0}^{\infty} \sigma_{Fl}(E), \tag{1.2}$$

where the partial wave cross section is given by

$$\sigma_{Fl}(E) = \pi \lambda^2 (2l+1) T_l(E). \tag{1.3}$$

Here λ is the reduced de Broglie wavelength of the projectile ion and $T_l(E)$ is the transmission coefficient for the lth partial wave. For all analytic calculations for fusion cross sections, one needs to calculate $T_l(E)$ very accurately.

For simplicity of theoretical calculations, Hill and Wheeler (HW) [20] suggested that the potential in the barrier region may be approximated by an inverted parabolic shape. In such a procedure, the parabola is fitted to reproduce the position, height, and the curvature of the real barrier and one obtains the analytic expression for the transmission coefficient. Parabolic barrier is a good approximation for energies above the top of the barrier. However, it is clear that this approximation is inadequate at energies well below the top of the barrier since the tail of the Coulomb interaction intersects the energy of the incoming particle at a point far away from the location of the potential maximum. To overcome this deficiency, Avishai [21] prescribed a model in which the $V_{\text{eff}}(r)$ is assumed to have two different forms on either side of the barrier top: the parabolic plus centrifugal barrier on the left and just the Coulomb potential between the two point charges on the right. A modification of Avishai's model was subsequently proposed by Dethier and Stancu [22] to take into account the centrifugal term on both sides of the barrier. This approximation leads to an analytic expression for $T_l(E)$ using the WKB method.

An interesting study of tunneling through a one-dimensional potential barrier appropriate for nucleus-nucleus fusion has been made recently by Ahmed [23]. He invoked a new parametrized potential barrier which admits simple WKB penetrability factor. His three parameter potential profile mimics the effective interaction potential barrier for almost the entire range of variable r (internuclear separation) as shown in Fig. 2. Thus it seems to be a good candidate for a satisfactory reproduction of experimental data. Furthermore, this potential resembles very well the Natanzon class of exactly solvable potentials [24] and hence is useful for comparing the semiclassical calculations for the transmission coefficient with the exact ones.

During the last decade, a new quantization procedure based on supersymmetric quantum mechanics (SUSYQM) [25] has emerged. The supersymmetry-inspired WKB (SWKB) quantization rule [26] not only yields exact bound state spectra from the leading order quantization formula for all shape-invariant potentials [27], but also gives frequently better results than the usual WKB method for non-shape-invariant potentials [28]. In case of tunneling through solvable one-dimensional barriers such as the Eckart, the SWKB method has been shown [29] to give much improved results for the transmission coefficient as compared to the WKB method. This feature encourages us to undertake the present investigation of BPM for fusion reactions in the context of SWKB method. Our motivation is not to suggest a new potential model for fusion processes but to demonstrate that SWKB procedure can predict accurate transmission coefficients and fusion cross sections working with the realistic potential model suggested by Ahmed. To the best of our knowledge, SWKB method has not so far been used to such a physically relevant and interesting area of nuclear physics.

In Sec. II we illustrate our method through the application to an exactly solvable one-dimensional potential barrier of the Natanzon class which resembles closely the profile of the actual fusion barrier. Comparison of SWKB transmission coefficient with the corresponding WKB results reveals that the present scheme is distinctly better than the conventional one. In Sec. III the SWKB method has been used to analyze the fusion excitation function of the reactions $^{16}O+^{12}C$, $^{19}F+^{12}C$, and $^{16}O+^{208}Pb$ and the values have been compared with the calculations based on HW and WKB approximations. For sub-barrier fusion for the light-heavy system, we display graphically our predicted results for $^{16}O+^{A}Sm$ along with the experimental data. Our results are substantially lower than the experimental values; this appears to be due to the deficiencies of the potential model considered in our analysis. Section IV is devoted to a short summary and conclusions.

II. SWKB METHOD FOR TUNNELING THROUGH A HYBRID POTENTIAL BARRIER

To begin with, we study the hybrid potential barrier belonging to the Natanzon class as suggested by Ahmed [23],

$$V(x) = V_0 \left[1 - \left(\frac{1-\exp(x/a)}{1+c\exp(x/a)} \right)^2 \right], \quad 0 \le c \le 1, \tag{2.1}$$

for which the Schrödinger equation admits exact analytic solution. It is interesting to note that for the limiting values of the parameter c, such as $c = 0$ and $c = 1$, the potential (2.1) corresponds, respectively, to the Morse $V(x) = V_0\{2e^{x/a} - e^{2x/a}\}$ and the Eckart $V(x) = V_0 \text{sech}^2(x/2a)$ barriers. In our earlier paper [29], we have discussed the SWKB approach for computing the transmission coefficient for the Eckart barrier. We, therefore, mention here only the salient steps for the general potential (2.1). For this purpose, we construct a pair of potentials

$$V^{(\mp)}(x,V_0)=W^2(x,V_0)\mp\frac{\hbar}{\sqrt{2m}}W'(x,V_0), \qquad (2.2)$$

where V_0 is the height parameter and $W(x,V_0)$ is the analytically continued superpotential function for the barriers. In other words, when one converts the barrier to well by replacing $V_0\to -V_0$, the corresponding $W(x,V_0)$ is related to the ground-state wave function of the $V^{(-)}(x,V_0)$ well. The SWKB transmission coefficients for these potentials are computed from the expression

$$T^{(\mp)}(E)=[1+\exp(2K^{(\mp)})]^{-1} \qquad (2.3)$$

where $K^{(\mp)}$ is the penetrability integral given by [29]

$$K^{(\mp)}=\frac{\sqrt{2m}}{\hbar}\int_{x_1}^{x_2}\sqrt{W^2(x,V_0)-E}\,dx\pm i\pi/2. \qquad (2.4)$$

Here x_1 and x_2 are the turning points satisfying the relation $W^2(x,V_0)=E$.

To recast the potential (2.1) in the form of $V^{(-)}(x)$, we begin with

$$V^{(-)}(x)=V_0\left[1-\left(\frac{1-\exp(x/a)}{1+c\exp(x/a)}\right)^2\right]+B \qquad (2.5)$$

where B is a constant. It may be seen that if we write a superpotential function

$$W(x)=\frac{\alpha e^{x/a}+\beta}{1+ce^{x/a}}, \qquad (2.6)$$

Eq. (2.5) can be written in the form of (2.2) if one sets the following parameters:

$$\alpha=[Bc^2+(c^2-1)V_0]^{1/2},$$
$$\beta=-\sqrt{B},$$
$$\Delta=\hbar^2/(2ma^2) \qquad (2.7)$$

with

$$B=\Delta\left[\frac{1-\{c^2-4(c+1)^2V_0/\Delta\}^{1/2}}{2(c+1)}\right]^2.$$

Using (2.6) in (2.4) and evaluating the integral [30] one gets the transmission coefficient for the barriers $V^{(\mp)}(x)$,

$$T^{(\mp)}(E)=\left[1+\exp\left\{\frac{2i\pi}{\sqrt{\Delta}}\left\{-[\beta+(\beta^2-E)^{1/2}]+\frac{1}{c}[\alpha-(\alpha^2-c^2E)^{1/2}]\right\}\pm i\pi\right\}\right]^{-1}. \qquad (2.8)$$

To obtain the transmission coefficient for the original potential (2.1) which differs from $V^{(-)}(x)$ in (2.5) only by a constant B, one requires to rescale the energy $E\to E+B$ in the expression of $T^{(-)}(E)$ in (2.8). One thus obtains the required transmission coefficient for the hybrid potential barrier (2.1)

$$T_{\rm SWKB}(E)=[1+\exp\{2\pi(g-s-f)\}]^{-1}, \qquad (2.9)$$

where

$$f=\sqrt{E/\Delta},$$
$$g=\left[\left(\frac{V_0}{\Delta}\right)\left(\frac{1}{c}+1\right)^2-\frac{1}{4}\right]^{1/2},$$
$$s=\left[f^2+\left(\frac{1}{c^2}-1\right)(V_0/\Delta)\right]^{1/2}. \qquad (2.10)$$

For the sake of comparison, we cite here also the exact and the WKB results [23]

$$T_{\rm exact}(E)=\frac{\sinh(2\pi f)\sinh(2\pi s)}{\cosh[\pi(g+s+f)]\cosh[\pi(f+s-g)]}, \qquad (2.11)$$

$$T_{\rm WKB}(E)=[1+\exp\{2\pi(g_W-s-f)\}]^{-1} \qquad (2.12)$$

with

$$g_W=(1/c+1)\sqrt{V_0/\Delta}.$$

Careful observation reveals that although the transmission coefficient in (2.9) looks very similar to the WKB result in (2.12), a few noticeable qualitative and quantitative differences arise due to the disappearance of the (1/4) factor in the definition of g_W as compared to g. These differences may be listed as follows:

(i) In the semiclassical limit when $\Delta\ll E, V_0$, the exact transmission coefficient in (2.11) tends to the analytic expression of $T_{\rm SWKB}(E)$, i.e.,

$$T_{\rm exact}(E)\approx T_{\rm SWKB}(E)\not\approx T_{\rm WKB}(E). \qquad (2.13)$$

(ii) The bound states of the well corresponding to the barrier in (2.1) can be obtained by analytic continuation procedure [31]. To achieve this, one has to change $V_0\to -V_0$ and $E\to -E_n$. These imply the following change of parameters:

$$f\to iF_n,\quad F_n=\sqrt{E_n/\Delta},$$

$$s\to iS_n,\quad S_n=\left[F_n^2+\left(\frac{1}{c^2}-1\right)(V_0/\Delta)\right]^{1/2}, \qquad (2.14)$$

$$g\to iG,\quad G=\left[(V_0/\Delta)\left(\frac{1}{c}+1\right)^2+\frac{1}{4}\right]^{1/2}$$

in $T_{\rm SWKB}$. The transmission function corresponding to the well is then given by

$$T = [1 + \exp\{2\pi i(G - S_n - F_n)\}]^{-1}. \tag{2.15}$$

Locating the poles of the transmission function on the upper half of complex k plane ($k = \sqrt{2mE}/\hbar$) one gets

$$F_n = G - S_n - (n + 1/2), \quad n = 0, 1, 2, \ldots . \tag{2.16}$$

The bound state energies can be easily obtained from (2.16),

$$E_n^{\rm SWKB} = -\Delta \left[\frac{(V_0/\Delta)(1/c^2 - 1) - [G - (n + 1/2)]^2}{2[G - (n + 1/2)]} \right]^2, \tag{2.17}$$

which is identical to the exact result given in Eq. (27) of Ref. [23]. This differs from the WKB result [obtained from Eq. (2.12) through similar inversion method]

$$E_n^{\rm WKB} = -\Delta \left[\frac{(V_0/\Delta)(1/c^2 - 1) - [g_W - (n + 1/2)]^2}{2[g_W - (n + 1/2)]} \right]^2 . \tag{2.18}$$

This distinctive feature of our method as compared to the WKB theory was reported earlier [29] for the special choice of $c = 0$ and 1 which correspond to the Morse and the Eckart barriers, respectively.

(iii) To identify the quantitative distinction of our calculation from the WKB approach, we compare numerically $T_{\rm SWKB}$ and $T_{\rm WKB}$ with $T_{\rm exact}$ for different values of the parameter c with fixed values of V_0 and a. For each value of c, we consider several values of the relative energy (E/V_0) of the incident particle so as to demonstrate the effect of sub-barrier and superbarrier penetrations. We take $V_0 = 3.0$ and $a = 0.5$ and the results are presented in Table I along with the percentage errors, shown in the last two columns. It is found that our SWKB formalism gives in general better results than the WKB method for wide variation of the parameter c ranging the potential (2.1) between two standard forms such as the Morse and Eckart barriers. In this respect, the present calculation may be considered as the generalization of our earlier work [29].

When the energy of the incident particle just grazes the top of the barrier, i.e., $E = V_0$, the WKB method leads to very large error for the transmission coefficient T for $c \approx 1$. This is clearly seen from Fig. 1 in which we display the variation of percentage error of the predicted transmission coefficients with the parameter c. It is interesting to note that while the error involved in the WKB method grows with increasing value of c and becomes about 33% for Eckart barrier ($c = 1$), the error associated with our SWKB approximation is minimal. In fact, it remains almost constant (at the level 0.5–1%) for the entire range of c.

III. APPLICATION TO HEAVY-ION FUSION

Presently we discuss the applicability of the SWKB method described in the previous section to a realistic potential that broadly describes the experimental data on light-light- and light-heavy-ion fusion processes. We consider the proximity potential of Blocki *et al.* modified by Baz and Alexander [32] for two colliding nuclei of atomic weight and mass numbers, (A_1, Z_1) and (A_2, Z_2),

$$V_F(r) = 4\pi\gamma b\tilde{C}(-3.437)\exp[-(r - C_1 - C_2)/0.75b] + \frac{Z_1 Z_2 e^2}{r} + l(l+1)\hbar^2/2mr^2 \tag{3.1}$$

with

TABLE I. Transmission coefficient (in units of $\hbar = 2m = 1$) for the hybrid potential in (2.1) with $V_0 = 3.0$ and $a = 0.5$ for different values of the parameter c and relative energy E/V_0. The exact, WKB, and SWKB results are computed from Eqs. (2.11), (2.12), and (2.9), respectively.

Parameter c	E/V_0	Transmission coefficient (T) Exact	WKB	SWKB	Percentage error WKB	SWKB
	0.1	0.01488	0.01285	0.01537	13.66	−3.20
	0.5	0.14741	0.12603	0.14747	14.50	−0.05
0.25	1.0	0.54536	0.50000	0.54537	8.32	−0.00
	1.5	0.85099	0.82641	0.85099	2.89	0.00
	2.0	0.95713	0.94901	0.95713	0.85	0.00
	0.1	0.00857	0.00654	0.00886	23.68	−3.20
	0.5	0.12005	0.09140	0.12010	23.86	−0.05
0.50	1.0	0.57569	0.50000	0.57570	13.15	−0.00
	1.5	0.89919	0.86796	0.89919	3.47	0.00
	2.0	0.97903	0.97176	0.97903	0.74	0.00
	0.1	0.00401	0.00279	0.00414	30.29	−3.21
	0.5	0.09081	0.06309	0.09085	30.53	−0.05
0.75	1.0	0.59743	0.50000	0.59744	16.31	−0.00
	1.5	0.92922	0.89844	0.92923	3.31	0.00
	2.0	0.98860	0.98317	0.98860	0.55	0.00

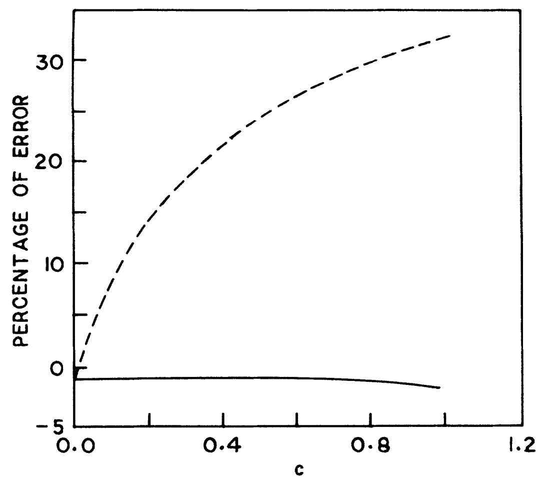

FIG. 1. Percentage error for the predicted transmission coefficient versus the parameter c for the hybrid potential (2.1) with $V_0 = 4.0$ and $a = 0.2$. We have taken the energy of the projectile grazing the top of the barrier, i.e., $E/V_0 = 1$ and $\hbar = 2m = 1$ throughout. The solid line and the dashed line correspond, respectively, to the present (SWKB) method [Eq. (2.9)] and WKB method [Eq. (2.12)].

$$\begin{aligned} \gamma &= 0.9517 \left[1 - 1.7826 \left(\frac{A-2Z}{A}\right)^2\right] (\mathrm{MeV/fm^2}), \\ R_i &= [1.28 A_i^{1/3} - 0.76 + 0.8 A_i^{-1/3} + \Delta R](\mathrm{fm}), \\ C_i &= [R_i - b^2/R_i](\mathrm{fm}), \\ \tilde{C} &= C_1 C_2/(C_1 + C_2). \end{aligned} \tag{3.2}$$

Here $A = (A_1 + A_2)$ and $Z = (Z_1 + Z_2)$ are the mass number and atomic number, respectively, of the composite system and ΔR is the modification of the effective sharp radius R_i. The surface width b in (3.1) has the approximate value 1 fm. Since the potential in (3.1) is not analytically solvable, the HW parabolic fitting [1] is often used to calculate the $T_l(E)$ which is directly related to the measurable quantity $\sigma_F(E)$. Except at the top of the barrier, the parabolic potential fails to account for the tail part of the effective fusion potential. For this reason, Ahmed has suggested a three-parameter potential barrier [23,33] which matches with the potential (3.1) for a suitable choice of the parameters. Furthermore, the parametrization is done in such a manner that the l-dependent centrifugal term is no longer needed. The potential is

$$V(r) = V_l \left[1 - \left(\frac{1 - \exp\{(r_l - r)/a\}}{1 - c\exp\{(r_l - r)/a\}}\right)^2\right] \tag{3.3}$$

with

$$a = d/(1-c),$$

$$d = [(\hbar^2/2m) 4 V_l/(\hbar\omega_l)^2]^{1/2},$$

$$\hbar\omega_l = \left[\frac{\hbar^2}{m}\frac{d^2 V_F(r)}{dr^2}\right]^{1/2}_{r=r_l}.$$

Here V_l is the maximum value of the barrier height and r_l is the position of the barrier top. We should emphasize here that all the parameters, V_l, r_l, a, c, and d are l dependent. Conventionally the s-wave peak value V_0 is called the Coulomb barrier height V_C. The HW frequency ($\hbar\omega_l$) takes care of the curvature near the top of the barrier and the parameter c fixes the position of the tail part of the potential. For the best matching of the two potentials in (3.1) and (3.3) over the entire range of r, we have required that both the potentials must have identical height as well as location of the peak. Also the tail portion has been matched at $r = 25$ fm. The extreme closeness of the analytic potential (3.3) and the fusion potential (3.1) can be seen from Fig. 2 for $^{19}F + ^{12}C$ system for the s wave ($l = 0$). The matching of these potentials has also been done for higher partial waves. The dependence of the parameters on the values of l for $^{19}F + ^{12}C$ can be seen from Table II. For illustration, we depict the optimum values of the parameters only for a few partial waves.

To apply our method to the potential (3.3), we follow the procedure stated in Sec. II. The potential can be recast in the standard SUSY form

$$V^{(-)}(r) = V_l \left[1 - \left(\frac{1 - \exp\{(r_l - r)/a\}}{1 - c\exp\{(r_l - r)/a\}}\right)\right] + D \tag{3.4}$$

where

$$D = \Delta \left[\frac{1 - \{c^2 - 4(c-1)^2 V_l/\Delta\}^{1/2}}{2(c-1)}\right]^2,$$

$$\Delta = \hbar^2/(2ma^2).$$

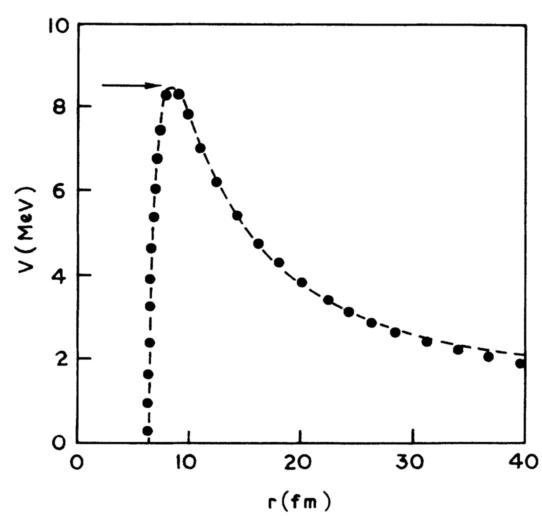

FIG. 2. The s-wave potential profile as a function of r for the $^{19}F + ^{12}C$ system. The dashed line represents our barrier model, Eq. (3.3), and the solid circles denote the experimental fusion interaction barrier given by Eq. (3.1). The arrow denotes the Coulomb barrier. The fitting parameters are $r_0 = 8.32$ fm, $V_0 = 8.50$ MeV, $\hbar\omega_0 = 2.65$ MeV, and $c = 1.062$.

The potential (3.4) can be obtained using (2.2) if one takes

$$W(r) = \frac{P\exp\{(r_l - r)/a\} + Q}{1 - c\exp\{(r_l - r)/a\}} \tag{3.5}$$

where

$$P = [Dc^2 + (c^2 - 1)V_l]^{1/2},$$

$$Q = -\sqrt{D}.$$

Using the superpotential function (3.5) in the transmission coefficient (2.3) and evaluating the penetrability integral [30], one gets

$$T_l^{(-)}(E) = \left[1 + \exp\left\{\frac{2\pi\varepsilon}{c\sqrt{\Delta}}[c(E - Q^2)^{1/2} + i\varepsilon(P + cQ) - (c^2E - P^2)^{1/2}] + i\pi\right\}\right]^{-1} \tag{3.6}$$

TABLE II. Parameters of the analytic potential (3.3) for several partial waves obtained by our matching procedure for the $^{19}F+^{12}C$ system.

l	r_l (fm)	V_l (MeV)	$\hbar\omega_l$ (MeV)	c
0	8.32	8.50	2.65	1.062
1	8.30	8.59	2.67	1.060
2	8.27	8.75	2.73	1.056
3	8.23	9.00	2.80	1.049
4	8.17	9.35	2.90	1.042
5	8.10	9.78	3.02	1.032
6	8.02	10.31	3.17	1.022
7	7.93	10.94	3.34	1.011
8	7.84	11.67	3.53	0.999
9	7.75	12.52	3.73	0.987
10	7.65	13.48	3.96	0.976

with

$$\varepsilon = \mathrm{sgn}(c - 1).$$

For obtaining the transmission coefficient for the potential (3.3), we rescale the energy $E \to (E + D)$ in (3.6) and obtain

$$T_l^{\mathrm{SWKB}} = [1 + \exp(2\pi\varepsilon[(E/\Delta)^{1/2} - \{(E/\Delta) + (1/c^2 - 1)(V_l/\Delta)\}^{1/2} - \varepsilon\{(1/c - 1)^2(V_l/\Delta) - 1/4\}^{1/2}])]^{-1}. \tag{3.7}$$

The corresponding expression for the WKB transmission coefficient as given in Ref. [23] is as follows:

$$T_l^{\mathrm{WKB}} = [1 + \exp(2\pi\varepsilon[(E/\Delta)^{1/2} - \{(E/\Delta) + (1/c^2 - 1)(V_l/\Delta)\}^{1/2} + (1/c - 1)(V_l/\Delta)^{1/2}])]^{-1}. \tag{3.8}$$

As before, our T_l^{SWKB} differs from T_l^{WKB} by a factor 1/4 appearing in the last term of (3.7).

Using the transmission coefficient in (3.7), we compute $\sigma_{Fl}(E)$ and $\sigma_F(E)$ for light-light and light-heavy nuclei.

TABLE III. Comparison of predicted fusion excitation function with measured data for $^{16}O+^{12}C$, $^{19}F+^{12}C$, and $^{16}O+^{208}Pb$ fusion reactions. Experimental data have been taken, respectively, from Refs. [5–7].

System	$E_{c.m.}$ (MeV)	E_{lab} (MeV)	$\sigma_F(E)$ (mb) HW	WKB	SWKB	Expt.
$^{16}O+^{12}C$	6.99	16.33	18.37	11.49	10.05	13.2±2.5
	7.99	18.63	99.23	90.91	82.65	80.5±8.5
$V_C = 7.88$	8.99	20.99	260.07	250.14	237.55	195±19
(MeV)	9.99	23.31	413.67	402.14	389.54	327±28
	11.99	27.98	634.56	623.80	612.84	540±46
	12.87	30.03	704.87	694.75	684.47	632±52
	13.99	32.63	777.96	768.62	759.12	773±60
$^{12}C+^{19}F$	19.4	50.0	1043.71	1036.88	1030.07	1040±15%
	24.5	63.2	1154.05	1148.73	1143.41	1150±15%
$V_C = 8.50$	29.4	76.0	1207.60	1203.19	1198.85	1070±15%
(MeV)	35.6	92.0	1239.45	1235.88	1232.38	
$^{16}O+^{208}Pb$	74.3	80	9.95	9.37	9.13	36±4
	77.1	83	101.42	100.59	99.48	108±10
$V_C = 75.36$	81.7	88	334.27	333.08	331.89	350±40
(MeV)	83.6	90	420.64	419.46	418.29	377±50
	89.1	96	655.24	654.12	653.00	685±70
	94.7	102	858.48	857.41	856.33	844±90
	120.0	129.6	1520.01	1519.13	1518.25	

It is crucial to decide how many partial waves really contribute meaningfully to a reaction process for a particular energy of the projectile. For this purpose, we refer to Fig. 34 of Ref. [4] in which the variation of $\sigma_{Fl}(E)$ with l for different system energies are displayed. We have also found that for energies far above the Coulomb barrier, σ_{Fl} increases almost linearly with l up to a value $l_{\max}$ since in this energy region $T_l(E) \approx 1$ due to the step-function-like behavior [29]. For l beyond certain maximum value $l_{\max}$, $V_l > E$ and T_l becomes nearly zero. Consequently, σ_{Fl} falls off sharply. For lower values of E, the maximum value of σ_{Fl} is reached for a lower value of l. In this domain, the quantal effect becomes prominent.

We have calculated the total fusion cross section for various systems but for the sake of brevity, we present in Table III our SWKB results only for a few typical reactions such as $^{16}O+^{12}C$, $^{19}F+^{12}C$, and $^{16}O+^{208}Pb$ for which reliable experimental data are available for both sub-barrier and above barrier penetration regions [5–7]. Our results are compared with those obtained from the WKB and the HW approximations. As expected, all three theoretical predictions are more or less comparable. However, for low Z_1Z_2 reactions, the SWKB predictions are closer to the measured data particularly for the energy below the Coulomb barrier. In these cases, the HW method overestimates $\sigma_F(E)$ due to the neglect of the Coulomb tail effect. A visual display of the calculated fusion cross section as a function of the energy of the projectile for the reaction of ^{16}O with even isotopes of Sm ($A = 148$ to 154) is presented in Fig. 3. Although the SWKB results are lower than the experimental values, the general trend of the variation is maintained over a wide range of the bombarding energy.

IV. CONCLUDING REMARKS

The main emphasis of the present investigation centered on the computability of the transmission coefficient for one-dimensional potential barrier using the newly emerging semiclassical (SWKB) technique. The barrier penetration model is quite popular for studying the broad features of nuclear fusion reactions as it gives a moderately good fit to the measured data. Before the work of Comtet *et al.*, it was customary to use either the Hill-Wheeler method or the WKB approximation to calculate the fusion cross section theoretically. With the advent of the supersymmetry-inspired WKB method which has been found to be quite successful in analyzing the bound state problems, it is believed that this scheme may work equally well in the continuum domain of the scattering processes. The present analysis certainly substantiates this hope and may motivate others to examine different processes involving tunneling phenomena.

Our work has proceeded in two steps: first, we have presented an illustrative calculation for the transmission coefficient for an analytically solvable hybrid potential which resembles closely the true fusion interacting barrier. We have been able to show that our SWKB method gives consistently better results than the WKB method both for sub-barrier and superbarrier penetrations and for the entire range of the free parameter c. This comparison has been possible due to availability of the exact expression for $T(E)$. One may therefore consider this part of the work as a model calculation for assessing the accuracy of the SWKB scheme. In the second part (Sec. III), we have shown how our method may be used to the realistic barrier problem in the context of heavy-ion fusion. It indicates the fact that although the SWKB transmission coefficient for one particular angular momentum quantum number may be superior than the corresponding WKB value, the cumulative effect in the total cross section (summed over all partial waves) is more or less the same for both the methods. But it is to be mentioned clearly that even then it is advantageous to use the SWKB method because it restores the correct energy eigenvalue spectrum from the transmission coefficient under the analytic continuation procedure through inversion of parameters as discussed in Sec. II.

Finally, we would like to remark that whatever discrepancies have been noticed between the SWKB predictions and the experimental data may be attributed to too simple a structure of the fusion potential (3.3) used for our analysis. It is now well established that fusion cross sections in heavy-ion reactions at energies near and below the Coulomb barrier are considerably enhanced over the predictions of the BPM model (see Fig. 3). In fact, the barrier penetration model neither accounts for the spin distribution of the fused composite systems, which is responsible for the sub-barrier fusion enhancement, nor considers the complex structure of the interacting nuclei such as the deformation of the nuclear shape, neck formation, etc., which are dominant effects in the sub-barrier region.

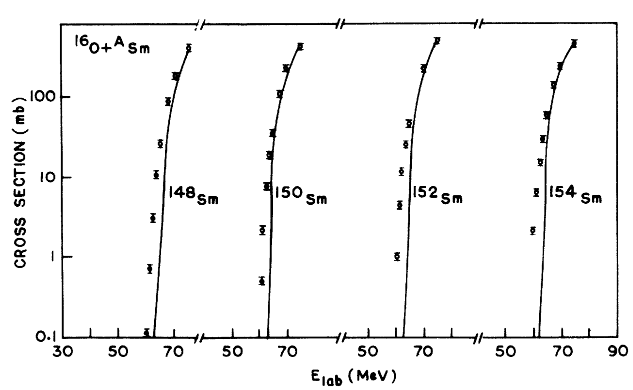

FIG. 3. Fusion cross sections predicted by the SWKB method (solid line) for ^{16}O and even isotopes of Sm ($A = 148$–154) are presented along with the experimental data (points with error bar) taken from Ref. [8].

ACKNOWLEDGMENTS

Two of us (T.S. and R.D.) wish to acknowledge the financial support received from the Department of Atomic Energy, Government of India. This work was also supported in part by a research grant from the Natural Sciences and Engineering Research Council of Canada to one of the authors (Y.P.V.).

[1] L. C. Vaz, J. M. Alexander, and G. R. Satchler, Phys. Rep. **69C**, 373 (1981), and references therein.
[2] D. M. Brink, *Semiclassical Methods for Nucleus-Nucleus Scattering* (Cambridge University Press, Cambridge, England, 1985).
[3] S. G. Steadman, *Fusion Reactions Below the Coulomb Barrier*, Lecture Notes in Physics Vol. 219 (Springer-Verlag, Heidelberg, 1985).
[4] M. Beckerman, Rep. Prog. Phys. **51**, 1047 (1988).
[5] Y. Eyal *et al.*, Phys. Rev. C **13**, 1527 (1976); B. Dasmahapatra, B. Cujec, and F. Lahlou, Nucl. Phys. **A384**, 257 (1982); Nucl. Phys. **A394**, 301 (1983).
[6] F. Puhlhofer, W. Pfeffer, B. Kohlmeyer, and W. F. W. Schneider, Nucl. Phys. **A244**, 329 (1975); B. Kohlmeyer, W. Pfeffer, and F. Puhlhofer, *ibid.* **A292**, 288 (1977).
[7] F. Videbaek *et al.*, Phys. Rev. C **15**, 954 (1977).
[8] D. E. DiGregorio *et al.*, Phys. Rev. C **39**, 516 (1989).
[9] R. A. Broglia and A. Winther, *Heavy Ion Reactions* (Benjamin, New York, 1981), Vol. 1.
[10] C. H. Dasso, S. Landowne, and A. Winther, Nucl. Phys. **A405**, 381 (1983); **A407**, 221 (1983); **A432**, 495 (1985).
[11] J. A. Christley, M. A. Nagarajan, and I. J. Thompson, J. Phys. G **17**, L163 (1991).
[12] Q. Haider and B. Cujec, Nucl. Phys. **A429**, 116 (1984).
[13] R. G. Stokstad *et al.*, Phys. Rev. Lett. **41**, 465 (1978); Phys. Rev. C **21**, 2427 (1980); D. E. Gregorio *et al.*, Phys. Lett. B **176**, 322 (1986).
[14] H. Esbensen, Nucl. Phys. **A352**, 147 (1980).
[15] U. Jahnke, H. H. Rossner, D. Hilsher, and E. Holub, Phys. Rev. Lett. **48**, 17 (1982).
[16] K. Siwek-Wilczynska and J. Wilczynski, Phys. Lett. **74B**, 313 (1978).
[17] A. K. Mohanty, S. V. S. Sastry, S. K. Kataria, S. Kailas, and V. S. Ramamurthy, Phys. Lett. B **247**, 215 (1990); A. K. Mohanty, S. V. S. Sastry, S. K. Kataria, and V. S. Ramamurthy, Phys. Rev. C **46**, 2012 (1992).
[18] H. Reeves, Astrophys. J. **146**, 447 (1966).
[19] J. Blocki, J. Randrup, W. J. Swiatecki, and C. F. Tsang, Ann. Phys. (N.Y.) **105**, 427 (1977).
[20] D. L. Hill and J. A. Wheeler, Phys. Rev. **89**, 1102 (1953).
[21] Y. Avishai, Z. Phys. A **286**, 285 (1978).
[22] J. L. Dethier and Fl. Stancu, Phys. Rev. C **23**, 1503 (1981).
[23] Z. Ahmed, Phys. Rev. A **47**, 4761 (1993).
[24] G. A. Natanzon, Theor. Mat. Fiz. **38**, 146 (1979); J. N. Ginocchio, Ann. Phys. (N.Y.) **159**, 467 (1985).
[25] E. Witten, Nucl. Phys. **B185**, 513 (1981); C. V. Sukumar, J. Phys. A **18**, 2917 (1985); O. D. Lange and R. E. Raab, *Operator Methods in Quantum Mechanics* (Clarendon, Oxford, 1991).
[26] A. Comtet, A. D. Bandrauk, and D. K. Campbell, Phys. Lett. **150B**, 159 (1985).
[27] A. Khare, Phys. Lett. **161B**, 131 (1985); R. Dutt, A. Khare, and U. P. Sukhatme, Phys. Lett. B **181**, 285 (1986); Am. J. Phys. **56**, 163 (1988); **59**, 723 (1991).
[28] F. Cooper, J. N. Ginocchio, and A. Khare, Phys. Rev. D **36**, 2458 (1987); R. Adhikari, R. Dutt, A. Khare, and U. P. Sukhatme, Phys. Rev. A **38**, 1679 (1988); P. Roy, R. Roychoudhury, and Y. P. Varshni, J. Phys. A **21**, 1589 (1988); Y. P. Varshni, *ibid.* **25**, 5761 (1992).
[29] T. Sil, A. Mukherjee, R. Dutt, and Y. P. Varshni, Phys. Lett. A **184**, 209 (1994).
[30] I. S. Gradshteyn and I. M. Ryzhik, *Tables of Integrals, Series and Products* (Academic, New York, 1965).
[31] J. N. Ginocchio, Ann. Phys. (N.Y.) **152**, 203 (1984); Z. Ahmed, Phys. Lett. A **157**, 1 (1991).
[32] L. C. Vaz and J. M. Alexander, Phys. Rev. C **18**, 2152 (1978).
[33] There is a minor printing error in Eq. (24) of Ref. [23]: the variable x will be $(r_l - r)/[d_l/(1 - c_l)]$.